Modeling and Analytical Study of Link Properties in Multihop Wireless Networks

Ming Zhao, *Student Member, IEEE,* Yujin Li, and Wenye Wang, *Member, IEEE*

***Abstract*—The radio link between a pair of wireless nodes is determined by radio channels, transmission range, node mobility and node-pair distance, which form a set of random factors in multihop wireless networks. The properties of such radio links can be characterized by link lifetime, residual link lifetime and link change rate, which, in fact, have been widely used for network design and performance evaluation. In this paper, we take a new modeling approach that captures the dynamics of radio channels and node movements in *small-scale*. More specifically, *distance transition probability matrix* is designed in order to describe the joint effects of dynamic transmission range due to radio channel fading and relative distance of a node-pair resulting from random movements. We find that the PDF of link lifetime can be approximated by an exponential distribution with parameter characterized by the ratio of average node speed $\bar{V}$ to *effective transmission range* R_e. To further understand the implication of link properties, analytical results are used to investigate the upper bound of network connectivity and the associated network performance is evaluated by extensive simulations.**

***Index Terms*—Ad hoc networks, mobility models, link dynamics, network connectivity, routing performance.**

I. Introduction

END-TO-END communications are carried out by a set of radio *links* between node pairs in multihop networks in which each node, except source and destination, behaves as a relay node to forward data packets to its next hop. Therefore, link properties are essential to applications and services in such networks because they have direct impacts on many performance metrics, such as end-to-end delay, packet losses, and throughput. Moreover, link properties, as fundamental characteristics of network dynamics, can also be used to design mobility-resilient multihop networks [2], [3], maximize routing performance[4], [5], optimize topology control[6]–[8], and achieve the desired network performance[9], [10].

However, our understanding of link properties is very limited, mainly because they are determined by a set of random factors, such as radio channels, dynamic transmission range, node mobility and node-pair distance in that there exists a *link* only a pair-node are within the transmission range of each other. Clearly, these random factors are closely dependent on time-varying radio environment and node mobility. Previous works have been focused on examining the effects of *node mobility* on link dynamics, such as link lifetime [3], [9], [11]–[13], link change rate [3], [14], link residual time and link availability [3], [13], [15], [16]. The main results include: i) Markovian model is an effective method to study relative movements and distance of a node-pair[12], [13]. (ii) There exists a peak in the link lifetime distribution based on random mobility models[3], [9], [11]. iii) The PDF of link change inter-arrival time can be approximated by an exponential distribution with fairly high accuracy[3], and iv) For a k-hop path, when k is very large, the path lifetime distribution converges to exponential distribution [17], whereas $k \geq 4$ for simulation results[9]. Specifically, the exponential parameter is the sum of the inverses of average link duration times [17].

Existing research on link properties falls into three categories: *simulation*-based, *experimental*-based, and *analysis*-based study. Extensive simulation-based studies [2], [9], [11], [18] have been performed to provide empirical distributions and statistical analysis of link lifetime and residual lifetime under different mobility models, including Random Waypoint (RWP), Random Walk (RW), Gauss-Markov (GM), Manhattan (MH) model, and Reference Point Group Mobility (RPGM) model. Another research methodology is to study *realistic* mobility models extracted from real traces, upon which inter-contact time properties between mobile users are widely studied in papers [19]–[21]. On the contrary, due to the complexity of node mobility, the breadth and depth of *analytical* studies on link properties are very limited.

The limitations of existing works on link properties are three-fold. First, existing random mobility models, such as RWP model and its variants, have significant drawbacks toward the steady-state properties of moving speed and nodal distribution, which could lead to defective analysis and simulations on link studies [2], [22]–[24]. Second, the time-scale of random mobility models (e.g., moving duration) is generally much larger than the time-scale of radio channels which may change rapidly and distinctly over short distance and time [7], [25]. However, the study in [26] suggested the time scale used to describe node mobility should be much smaller than the time scale for capturing the significant channel variability. Third, it is assumed in previous studies that transmission range of each node is a constant, which is helpful in simplifying the analysis, at the cost of ignoring the effect of radio environments. For instance, Bettstetter provided a wireless channel model and studied how shadow fading affects the topology and connectivity of multihop wireless networks[6]. Correspondingly, in [26], the authors showed that the relative movement of the transmitter-receiver pair can

Paper approved by B. Sikdar, the Editor for Wireless Packet Access and Cross-Layer Design of the IEEE Communications Society. Manuscript received November 28, 2009; revised May 11, 2011.

Parts of this paper appeared in the Proc. of IEEE INFOCOM 2008 [1].

This work is supported by NSF CCF-0830680 and NSF CNS-1018447.

The authors are with the Department of Electrical and Computer Engineering, North Carolina State University, Raleigh, NC 27695 (e-mail: {mzhao2, yli27, wwang}@ncsu.edu).

Digital Object Identifier 10.1109/TCOMM.2012.010512.090739

cause significant channel variability, due to the time-varying multi-path propagation, mobility and multiuser interference. Therefore, considering both radio environments and node mobility at similar time-scale is critical to better, or even correctly understanding link and path properties in multihop wireless networks. Therefore, we aim to study the link properties regarding these two independent, yet simultaneously forcible factors (radio channels and smooth node mobility). Our approach is to use a *distance transition probability matrix* for modeling the node-pair distance after every discrete time step based on a *smooth mobility model* which captures the *small-scale* variation in relative distance [24]. By examining the relationship between time-varying transmission range and node-pair distance, we will be able to study link properties.

Somewhat surprisingly, we show that link lifetime distribution can be effectively approximated by an exponential distribution, which is in contrast to previous results that there exists a peak in the distribution function which are mainly obtained from random mobility models [3], [9], [11]. More interestingly, the exponential distribution parameter can be simplified by $\frac{\bar{V}}{R_e}$, where $\bar{V}$ is the average speed and R_e is the effective transmission range (ETR) of a mobile node. Since the path lifetime is determined by the minimum link lifetime en route, we can easily conclude that the PDF of path lifetime also follows an exponential distribution, which greatly relaxes the assumption of large (approach to infinite) hop-count of a path for its distribution converging to exponential [17]. We also find that the impacting factors on both link and residual link lifetime are in the decreasing order of average node speed, ETR, and node-pair distance.

The remainder of the paper is organized as follows. Section II presents the characterization of radio links by effective transmission range with radio channel fading, and by node mobility with smooth node mobility model and node-pair distance. We present the models and analysis for understanding link lifetime distribution in Section III, and other link properties in Sections IV. The implication of link properties are studied in Section V in which k-hop path properties, network connectivity, and routing protocols based on these derived link and path properties are discussed. Finally, Section VI concludes the paper.

II. Characterization of Radio Links and Mobility

As the optimal and fixed radio transmission range are rarely achieved in real dynamic wireless channels, we introduce the concept of *effective transmission range* (ETR) by using radio fading models [7], which is simple, yet can characterize radio propagation, i.e., *path loss*, *shadowing effect*, and *multi-path fading* of wireless links [25]. Hence, the link lifetime between a pair of nodes is determined concurrently by ETR and node-pair distance over-time upon smooth node mobility [24].

A. Effective Transmission Range

In mobile radio environments, the received signal is generally influenced by three fading effects: large-scale path loss, multi-path fading, and shadowing [25]. For instance, in vehicular movements, mobile nodes usually move at high speeds, so that the *large-scale path loss*, can be the dominant factor affecting the signal strength with increasing distance. On the other hand, the relative movement of two persons inside a building may be over a short travel distance (order of wavelengths), which is mainly constrained by *small-scale* fading, also called multi-path fading. Due to the presence of obstacles in the propagation channel, the signal also undergoes *shadowing* loss. More over, in [27], it is showed that the link and connectivity analysis given the geometric disc abstraction holds for more irregular shapes of a node transmission zone. Therefore, we introduce a novel metric, *Effective Transmission Range* (ETR), to capture the effect of radio propagation mechanisms.

Definition 2.1: In a radio channel characterized by the path loss exponent ξ, shadowing X_{σ_s} and multi-path fading χ^2, *Effective Transmission Range* (ETR), denoted by R_e, is the maximum value of the transmission range R, which holds the condition $P_{r,dB} \geq P_{0,dB}$ with a very high probability (w.h.p.) $\mathbb{P} = 99\%$, where $P_{r,dB}$ is the received signal power and $P_{0,dB}$ is the threshold of the receiving power.

Let $\tilde{P}_{dB} = P_{t,dB} - \overline{L}_{0,dB} - 10\log_{10} E\{\chi^2\}$, where $P_{t,dB}$ is the transmission power, and $\overline{L}_{0,dB}$ is the average path loss at the reference point that is 1 meter away from the transmitter. $10\log_{10} E\{\chi^2\}$ is the average multi-path fading in dB [25]. The probability $\mathbb{P}$, i.e. $Pr\{P_{r,dB} \geq P_{0,dB}\}$ is represented as:

$$\begin{aligned}\mathbb{P} &= Pr\{\tilde{P}_{dB} - 10\xi\log_{10} R_e - X_{\sigma_s} \geq P_{0,dB}\} \\ &= \frac{1}{\sqrt{2\pi}\sigma_s}\int_{-\infty}^{\tilde{P}_{dB}-10\xi\log_{10} R_e - P_{0,dB}} exp(-\frac{x^2}{2{\sigma_s}^2})dx \\ &= \frac{1}{2}[1 - erf(\frac{10\xi\log_{10} R_e + P_{0,dB} - \tilde{P}_{dB}}{\sqrt{2}\sigma_s})], \qquad (1)\end{aligned}$$

where $erf(\cdot)$ is the error function, defined by $erf(z) = \int_0^z \frac{2}{\sqrt{\pi}} e^{-x^2} dx$. From the Definition 2.1, we have

$$\begin{cases} \frac{1}{2}[1 - erf(\frac{10\xi\log_{10} R_e + P_{0,dB} - \tilde{P}_{dB}}{\sqrt{2}\sigma_s})] = \mathbb{P} = 0.99, \\ \frac{10\xi\log_{10} R_e + P_{0,dB} - \tilde{P}_{dB}}{\sqrt{2}\sigma_s} = -1.65. \end{cases} \qquad (2)$$

Hence, upon (2), we obtain the ETR, denoted by R_e, of mobile nodes with specific requirements in a radio environment:

$$\log_{10} R_e = \frac{-2.33\sigma_s + \tilde{P}_{dB} - P_{0,dB}}{10\xi}. \qquad (3)$$

For simplification, we assume that certain mobile nodes use the same transmission and receiving power threshold, then $P_{t,dB} - \overline{L}_{0,dB} - P_{0,dB}$ is a constant value denoted by c. From (3), we find that R_e can written as a function of three fading parameters:

$$R_e = f(\xi, \sigma_s, \chi) = 10^{\frac{-2.33\sigma_s - 10\log_{10} E\{\chi^2\} + c}{10\xi}}. \qquad (4)$$

As an illustration, from (4), we find that an increase of 1 dB in either σ_s or $E\{\chi^2\}$ only, R_e will be decreased by 16% and 7%, respectively; when path loss exponent ξ increases by 1, e.g. from 3 to 4, R_e will decrease around 30%.

Remark 1: The impacting weight of channel fading on ETR is in the decreasing order of path loss (ξ), shadow fading (X_{σ_s}), and multi-path fading (χ^2).

The introduction of ETR concept has several advantages. First of all, R_e is able to capture the effect of radio channel parameters such as path-loss, shadowing, and multi-path fading.

The effect of any one of these parameters can be found through the close-form of analytical results in terms of R_e. Second, R_e provides an easy method to characterize radio channels. For instance, Definition 2.1 and (1) can be further extended to include other factors such as coding schemes, power-control, and bit error rates. Finally, by taking R_e as a given value during the derivation, the analysis can be greatly simplified, while the results, in fact, can be considered as *conditioned* on R_e. This empowers us to focused on the models and approaches instead of detailed derivation.

B. Smooth Mobility Model

Many studies have shown that node mobility has significant impact on link properties in multihop wireless networks [2], [3], [9], [14], [28]. Therefore, the mobility model selected for studying link dynamics is critical to the results. It is worth noting that the time-scale of wireless channels is closely dependent on radio propagation. In particular, the path loss is the function of distance, and does not vary with time. In contrast, the multi-path fading changes within small distance and the fading changing rate is proportional to the receiver velocity. Hence, multi-path fading changes in the order of seconds [25]. Note that, in indoor environments, mobile nodes are often connected via wireless access points rather than through multi-hop networks. Hence, in this study, we focus on mobile users in outdoor environments, in which the shadow fading varies with travel distance of a mobile user at the order of tens or hundreds of meters. That indicates that the radio channel variation time relies on the node speed within a short time interval. Therefore, in order to observe the concurrent influence of radio channels and mobility on link lifetime, we must consider the characteristics of node mobility in the similar time-scale of radio channels. Specifically, the mobility model should satisfy the following requirements:

1. Since the signal strength may change rapidly and distinctly over short travel distance and short time [7], [25], the mobility model need to describe the minute variation of node velocity in small time-scale, by which the up-to-date information of relative movement between two nodes can be easily obtained.

2. To comply with the physical law of a smooth motion, the mobility model should capture the temporal correlation of node velocities with smooth speed and direction transition in each movement [22], which results in the frequent variation of relative speed between two nodes during the link connection.

Among existing mobility models [22], [24], the *smooth* mobility model proposed in [24] is chosen as a benchmark because this model allows flexible, *small* equal-length time steps (Δt) for smooth movement description. First of all, with movement update interval at *microscopic* level, the smooth mobility is suitable for study of high dynamic radio channel and link properties. Second, the model complies with the physical law of smooth motion: each movement in the smooth model contains three consecutive moving phases: Speed Up phase, Middle Smooth phase, and Slow Down phase. Node accelerates its speed to the target speed of the movement initially, updates velocity and direction with *temporal correlation* with those at previous step during Middle Smooth phase, and decelerates speed before a full stop. Furthermore, the model has nice steady-state properties of uniform nodal distribution for analysis and stable moving speed for simulation verification[1]. These nice properties provide us realistic smooth mobility model with movement update at microscopic level, which is crucial to analyze link dynamics.

C. Node-Pair Distance

The distance between two mobile nodes is denoted by *Node-Pair Distance*, ρ, which is dependent on the relative movements of two nodes. For instance, ρ_m represents the distance between two nodes after m time steps. As an example, Fig. 1(a) illustrates the relationship between the maximum transmission range $R_{\max}$ and node-pair distance ρ_m under different radio environments. Thus, by comparing the value between the time-varying variable $R_{\max}$ and ρ_m at each time step (normalized to 1 second per time step Δt), the corresponding link existence can be obtained, which is shown in Fig. 1(b). For example, as shown in Fig. 1(a), if only consider large-scale path loss, the ETR is considered to be constant of 200 m, hence the link between two nodes is connected as long as their relative distance is less than 200 m. While as consider the other two fading, the ETR transits dramatically within seconds. By comparing the relative distance and the ETR, Fig. 1(b) illustrates the link lifetime between two mobile nodes with respect to different channel fading. It is evident that the link lifetime is much shorter and the link breaks much more frequently when either shadowing or multi-path or both fading effects are considered.

Based on this illustration, the frequency of link breakage under all three fading is 19 times larger than that with path loss only and 7 times larger than that with both path loss and shadowing. And their impacts on average link lifetime is based on the reverse ratio of that on the link breakage rate.

As shown in Fig. 1(a), given a specific radio environment, the maximum transmission range $R_{\max}$ between two nodes varies dramatically with time. Accordingly, the effective transmission range R_e, defined in (3), can efficiently characterize the valid transmission distance with specific radio fading. In fact, the similar concept of ETR has been already applied in the real industrial world. For example, the Accutech wireless instrumentation products use $1/3$ of the maximum transmission range $R_{\max}$ as the rule-of-thumb for working transmission range [29].

Remark 2: For a pair of nodes (u, w), there exists a link between them if and only if their distance ρ_m is no greater than their symmetric effective transmission range R_e.

Thus, the link lifetime T_L, in essence, is defined as

$$T_L \triangleq \sup_{m>0}\{m \cdot \Delta t : \rho_i \le R_e, \forall i, 1 \le i \le m\}. \qquad (5)$$

Note that the node-pair distance ρ_m is a random variable, which is dependent on node mobility. Although node-pair distance or velocity can be easily measured by GPS type of tools, these types of data set usually represent specific network scenarios, such as down-town cabs or buses movement

[1]More details about steady-state properties of mobility models can be found in [24]

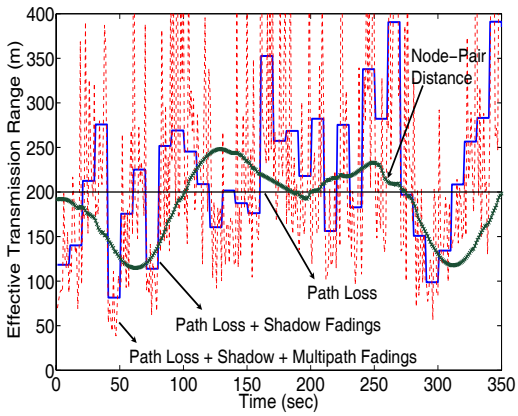

(a) Effective transmission range.

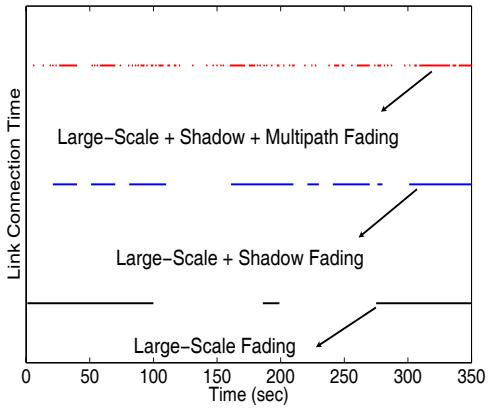

(b) Comparison of link lifetime.

Fig. 1. Illustration of ETR vs. link lifetime under different radio channels, where node speed is 2 m/sec.

traces. Hence experimental measurement based on localization methods, such as GPS, is insufficient for deriving general distribution of node-pair distance such as to analyze link lifetime distribution. In the next section, we start with the relative movement of a node-pair upon smooth mobility model, and then we derive the link lifetime distribution.

III. Link Lifetime Distribution

Fundamental link properties can be analyzed by link lifetime, residual link lifetime, and link change rate. In fact, *link lifetime* is random variable, which is defined as the time from a link appears between a node-pair to the moment this link is broken. The probability distribution function (PDF) of link lifetime demonstrates the basic link property, and can be used to analyze other properties as shown later in Section IV. In this section, we propose a new modeling approach for the analysis by several steps: find the relative speed and relative distance first, then define a *transition probability matrix* to model the distance transition at each time step, followed by the derivation of link lifetime distribution.

A. Relative Movement: Speed and Distance

For a node-pair (u, w), we use node u as the reference node, which lies in the center of its transmission zone with radius of the effective transmission range R_e. As explained in previous section, we use the smooth mobility model [24] in order to match the time-scale variation of radio channels [26] and smooth motion of moving nodes. Thus, the relative distance of a node-pair can be represented by relative positions at each time step. An example of the relative movement trajectory is illustrated in Fig. 2. We denote v_m as the magnitude of the relative speed vector $\overrightarrow{v}_m$. After the m^{th} time step relative movement, node w lies at the position represented by (X_m, Y_m). Correspondingly, ρ_m, the node-pair distance, is the magnitude of the vector $\overrightarrow{\rho}_m$, such that $\rho_m = \sqrt{{X_m}^2 + {Y_m}^2}$. We assume that the relative speed v_m and the angle ψ_m of node w are i.i.d. RVs, then the coordinate X_m and Y_m can be approximated by Gaussian random distribution, when $m >> 1$ [15]. For simplicity, we normalize the time step unit Δt to 1 second throughout the rest of the paper, then the m^{th} step relative speed v_m is:

$$v_m = |\overrightarrow{v}_m| = \sqrt{(X_m - X_{m-1})^2 + (Y_m - Y_{m-1})^2}, \qquad (6)$$

where both RV $(X_m - X_{m-1})$ and $(Y_m - Y_{m-1})$ can be effectively approximated by an identical Gaussian distribution with zero mean. Thus, upon the same arguments in [15], when $m >> 1$, v_m can be further effectively approximated by a *Rayleigh density* represented as [30]:

$$f_Z(z) = \frac{z}{\alpha^2}\, e^{\frac{-z^2}{2\alpha^2}} U(z) \quad \text{and} \quad E\{z\} = \alpha\sqrt{\pi/2}, \qquad (7)$$

where α is the parameter of the Rayleigh distribution. To simplify the analysis, we assume that mobile nodes have the same average moving speed $\bar{V}$, though with different mobility pattern. Then the range of relative speed of two nodes is over $[0, 2(\bar{V} + \delta_V)]$, depending on either two node moving along the same direction or the opposite direction, where δ_V is the maximum speed deviation of $\bar{V}$ in one movement introduced in the smooth model. Upon (7), $\bar{V} = \alpha\sqrt{\pi/2}$, then the PDF of relative speed is:

$$f_V(v) = \frac{v}{(\bar{V}\sqrt{\frac{2}{\pi}})^2}\, e^{\frac{-v^2}{2(\bar{V}\sqrt{\frac{2}{\pi}})^2}} = \frac{\pi v}{2\bar{V}^2}\, e^{\frac{-\pi v^2}{4\bar{V}^2}}. \qquad (8)$$

To validate the expression in (8), we obtain the relative speed distribution $f_V(v)$ between two nodes by simulations under smooth mobility with different levels of node speed. More specifically, the mobile node increases speed evenly from 0 m/sec to a targeting speed during speed up phase. Accordingly, the mobile node decreases speed evenly to 0 m/sec during slow down phase. Note that, mobile node will not change direction at speed up phase and slow down phase either. In Middle Smooth phase, mobile node can change speed and direction with 0.5 correlation of previous speed and direction. Each phase includes random number of time steps from the range [6,30] with a uniform probability, where each time step is one second. The targeting speed for a mobile node is selected from 2, 5, 10, 15, 20 m/sec. Five runs are simulated against each targeting speed level, in which 50 mobile nodes move at the same targeting speed in a 1041 m * 1041m simulation area for 1000 seconds.

Fig. 3 illustrates the PDF of relative speed resulted from both simulation and the theoretical expression from (8) versus different values of $\bar{V}$ as $[2, 5, 10, 15, 20]$ m/sec, respectively. It

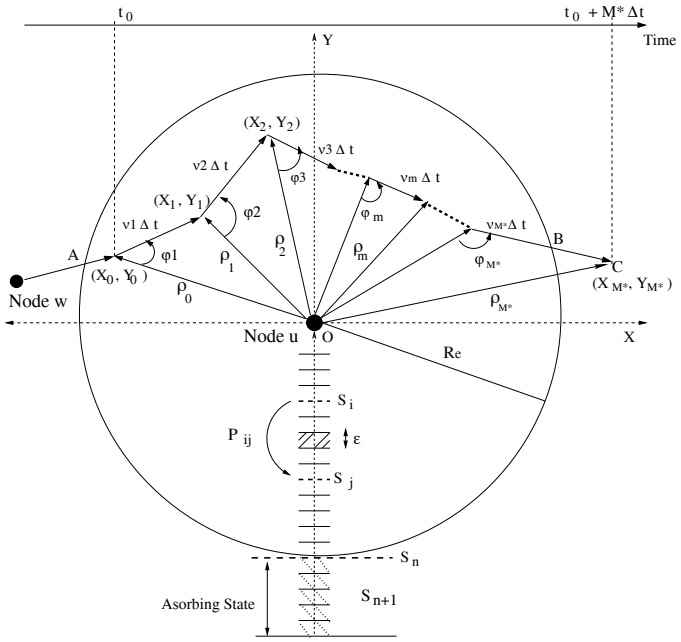

Fig. 2. Relative movement trajectory of node-pair (u, w).

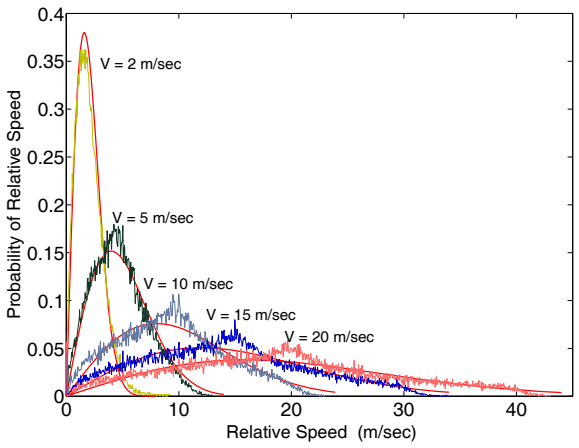

Fig. 3. Rayleigh distribution approximation of the relative speed.

can be observed that the approximated Rayleigh distribution matches very well with the distribution of relative speed obtained by simulations.

Remark 3: The relative speed of a node-pair can be approximated by Rayleigh distribution not only for large-scale mobility [15], but also for small-scale smooth mobility. In fact, the smaller the time step of mobility modeling is, the more accurate the approximation yields.

As illustrated in Fig. 2, ρ_m is a random variable that depends on the current and next positions of node w in relation to node u. Specifically, at the m^{th} step, $\overrightarrow{\rho}_m = \overrightarrow{\rho}_{m-1} + \overrightarrow{v}_m$. Hence, ρ_m can be represented as:

$$\rho_m = |\overrightarrow{\rho}_m| = \sqrt{\rho_{m-1}^2 + {v_m}^2 - 2\rho_{m-1} v_m \cos\psi_m}, \qquad (9)$$

where ψ_m is uniformly distributed from $[0, \pi)$. From (9), ψ_m can be represented as:

$$\psi_m = \arccos \frac{{\rho_{m-1}}^2 + {v_m}^2 - {\rho_m}^2}{2\rho_{m-1} v_m}. \qquad (10)$$

We denote $f_{\rho_m|\rho_{m-1}}(\rho_m \mid \rho_{m-1})$ as the conditional distribution of relative distance, which is given by

$$\begin{aligned} & f_{\rho_m|\rho_{m-1}}(\rho_m \mid \rho_{m-1}) \\ = & \int_0^{2(\bar{V}+\delta_V)} f_{\rho_m|\rho_{m-1},v_m}(\rho_m \mid \rho_{m-1}, v_m) \cdot f_V(v_m) dv_m \\ = & \int_0^{2(\bar{V}+\delta_V)} \frac{\frac{2}{\pi}\rho_m \cdot f_V(v_m) dv_m}{[4\rho_{m-1}^2 {v_m}^2 - ({\rho_{m-1}}^2 + {v_m}^2 - {\rho_m}^2)^2]^{1/2}}, \end{aligned} \qquad (11)$$

where $f_V(v)$ is the PDF of the relative speed. Thus, the conditional probability of node-pair distance can be determined by substituting $f_V(v)$ obtained from (8) into (11). The result of (11) is useful in understanding the transition between two consecutive steps. However, it is not sufficient to know the node-pair distance at an arbitrary time instant, which is a time-varying variable. In order to examine the node-pair distance at each time step, the effective transmission range R_e of node u is quantized into n equal-length intervals with a width of ε meters. Hence, $R_e = n \cdot \varepsilon$, which indicates that there are n states within the transmission zone. Each interval ε is associated with a state representing the u-w distance. For example, state S_i indicates that the u-w distance interval is over the range $[(i-1)\varepsilon, i\varepsilon]$, which is shown in the lower half in Fig. 2. Note, since ε is a unit of distance interval, the number of states n is a variable in proportion to R_e, which is in turn characterized by the wireless environment.

B. Distance Transition Matrix $\mathbf{P}$

We denote $\mathbf{P}$ as the distance transition probability matrix, to model the distance transition at each time step. Each element P_{ij} indicates the transition probability that u-w distance is changed from current state S_i to next state S_j after one time step. From Fig. 2, the link expires after the M^{*th} time step when the event of $\{\rho_{M^*} > R_e\}$ first happens. In addition, we use state S_{n+1} to represent all the u-w distances that are greater than R_e. Since link connection breaks when node w reaches state S_{n+1}, we define state S_{n+1} as the *absorbing state* of matrix $\mathbf{P}$. This implies that $\mathbf{P}$ is an n by $n+1$ matrix. The value of P_{ij} of matrix $\mathbf{P}$ is essential to the analytical study of link dynamics. The details of how to find the link lifetime distribution by using $\mathbf{P}$ will be explained in Section III-C. Next, we derive the approximation of P_{ij} based on node-pair distance distribution in (11).

First, the transition probability P_{ij} can be represented by:

$$\begin{aligned} & P_{ij} = Prob\{\rho_m \in S_j \mid \rho_{m-1} \in S_i\} \\ = & \frac{Prob\{(j-1)\varepsilon \le \rho_m \le j\varepsilon \ \cap \ (i-1)\varepsilon \le \rho_{m-1} \le i\varepsilon\}}{Prob\{(i-1)\varepsilon \le \rho_{m-1} \le i\varepsilon\}} \\ = & \frac{\int_{(j-1)\varepsilon}^{j\varepsilon} \int_{(i-1)\varepsilon}^{i\varepsilon} f_{\rho_m|\rho_{m-1}}(\rho_m|\rho_{m-1}) f(\rho_{m-1}) d\rho_{m-1} d\rho_m}{\int_{(i-1)\varepsilon}^{i\varepsilon} f(\rho_{m-1}) d\rho_{m-1}}. \end{aligned} \qquad (12)$$

It is clear that (12) can be obtained by substituting (11) into it. However, we find the result of such an expression of (12) cannot be simplified to a closed-form representation and

is too complicated for computation. Thus, we aim to derive an approximation of P_{ij} for easy analysis.

Theorem 1: The transition probability P_{ij} of matrix $\mathbf{P}$ can be approximated by

$$\begin{cases} \tilde{P}_{ij} \approx \frac{0.2\varepsilon}{\bar{V}}\sqrt{\frac{2j-1}{2i-1}}\Big[\ln\frac{|4(\bar{V}+\delta_V)^2-\varepsilon^2(j-i)^2|(i+j-1)^2}{|\varepsilon^2(i+j-1)^2-4(\bar{V}+\delta_V)^2|(j-i)^2}\Big]^{\frac{1}{2}} \\ P_{ij} = \tilde{P}_{ij}/\sum_j \tilde{P}_{ij} \quad \forall i. \end{cases} \tag{13}$$

Recall that $\bar{V}$ represents average node speed and δ_V is the maximum variation of $\bar{V}$ according to smooth model [24].

Proof: Let $f(x) = e^{\frac{-\pi x}{4\bar{V}^2}}$ and $g(x) = \Big[4\rho_{m-1}^2\rho_m^2 - \big[x-(\rho_{m-1}^2+\rho_m^2)\big]^2\Big]^{-1/2}$. With (11), we can see that $f(x)>0$ and $g(x)>0$, when $x\in[0,4(\bar{V}+\delta_V)^2]$. By using *Schwartz inequality* [30],

$$\int_a^b |f(x)\cdot g(x)|dx \le \Big[\int_a^b |f(x)|^2dx\Big]^{\frac{1}{2}}\Big[\int_a^b |g(x)|^2dx\Big]^{\frac{1}{2}}. \tag{14}$$

we have

$$f_{\rho_m|\rho_{m-1}}(\rho_m \mid \rho_{m-1}) \le \frac{\rho_m}{2\bar{V}^2}\Big[\int_0^{4(\bar{V}+\delta_V)^2} e^{\frac{-\pi x}{2\bar{V}^2}}dx\Big]^{\frac{1}{2}} \times \Big[\int_0^{4(\bar{V}+\delta_V)^2} \frac{dx}{4\rho_{m-1}^2\rho_m^2-\big[x-(\rho_{m-1}^2+\rho_m^2)\big]^2}\Big]^{\frac{1}{2}}. \tag{15}$$

Then by respectively deriving the integral of $f(x)$ and $g(x)$, plus a bit work on simplification, the approximation of the conditional distribution $f_{\rho_m|\rho_{m-1}}(\rho_m \mid \rho_{m-1})$ can be:

$$f_{\rho_m|\rho_{m-1}}(\rho_m \mid \rho_{m-1}) \le \frac{0.2}{\bar{V}}\sqrt{\frac{\rho_m}{\rho_{m-1}}} \times \Big[\ln\frac{|4(\bar{V}+\delta_V)^2-(\rho_m-\rho_{m-1})^2|(\rho_{m-1}+\rho_m)^2}{|(\rho_{m-1}+\rho_m)^2-4(\bar{V}+\delta_V)^2|(\rho_m-\rho_{m-1})^2}\Big]^{\frac{1}{2}}. \tag{16}$$

We further apply the Mean-Value theorem to derive the numerical solution of P_{ij}. In particular, according to P_{ij} defined in (12), where $(j-1)\varepsilon \le \rho_m \le j\varepsilon$ and $(i-1)\varepsilon \le \rho_{m-1} \le i\varepsilon$, if ε is sufficiently small, we can effectively use the middle point $i-\frac{\varepsilon}{2}$ and $j-\frac{\varepsilon}{2}$ to respectively represent the value of ρ_{m-1} and ρ_m [13]. For instance, $\int_{(i-1)\varepsilon}^{i\varepsilon} f(\rho_{m-1})d\rho_{m-1} \approx \varepsilon\cdot f(i\varepsilon-\frac{\varepsilon}{2})$. With this argument and the result from (16), P_{ij} derived in (12) can be effectively approximated by $\tilde{P}_{ij}$:

$$\tilde{P}_{ij} \approx \varepsilon\cdot f_{\rho_m|\rho_{m-1}}[(j-\frac{1}{2})\cdot\varepsilon \mid (i-\frac{1}{2})\cdot\varepsilon)] \tag{17}$$

By using the results from (16) and (17), we can obtain $\tilde{P}_{ij}$ as shown in Theorem 1. Note, the approximation value of $\tilde{P}_{ij}$ is normalized along each row of the matrix $\mathbf{P}$ to guarantee the fundamental property of the transition matrix $\mathbf{P}$, i.e., $\sum_j P_{ij}=1,\ \forall i, 1\le i\le n$, as shown in (13). ∎

C. Approximation of Link Lifetime Distribution

Upon Fig. 2, a communication link between a node-pair forms immediately after the node w crosses the border of node u's transmission zone at time t_0. Recall that T_L denotes the link lifetime, which is the time node w continuously lies inside node u's transmission zone. The link expires after the M^{*th} time step when the node-pair distance is larger than ETR for the first time since t_0. In this example, $T_L = M^*\Delta t$, hence T_L is a random variable from (5) and the CDF of link lifetime is $Prob\{T_L \le m\}$ for $\Delta t = 1$ s.

Here, we derive the link lifetime distribution based on the distance transition matrix $\mathbf{P}$ obtained in previous subsection. We denote by $\pi_i^{(m)}$ the probability that node w lies in state S_i after the m^{th} step, and $\pi^{(m)}$ is the row vector whose i^{th} element is $\pi_i^{(m)}$. That is $\pi^{(m)} = \Big(\pi_1^{(m)},\cdots,\pi_i^{(m)},\cdots,\pi_{n+1}^{(m)}\Big)$. And $\pi^{(0)}$ denotes the probability of the initial state that node w lies when the link is initially formed, for instance, according to illustration in Fig. 2, at time t_0, $\pi_i^{(0)} = Prob\{\rho_0 \in S_i\}$. For simplicity, we denote matrix $\mathbf{P}$ as $\mathbf{P} = [P_1,\cdots,P_j,\cdots,P_{n+1}]$ and P_j is the j^{th} column vector of $\mathbf{P}$. That means,

$$P_j = [P_{1j}, P_{2j},\cdots,P_{ij},\cdots,P_{(n+1)j}]^T, \tag{18}$$

where P_{ij} is obtained from Theorem 1 in (13).

Because S_{n+1} is the absorbing state of the matrix $\mathbf{P}$, $[\pi^{(0)}\mathbf{P}^m]_{(n+1)}$ represents the probability that node w moves outside node u's transmission zone within m time steps. Then the CDF of link lifetime can be obtained by:

$$\begin{aligned} &Prob\{T_L \le m\} = Prob\{\rho_m > R_e | \rho_0 \le R_e\} \\ &= [\pi^{(0)}\mathbf{P}^m]_{(n+1)} = \pi_{n+1}^{(m)}. \end{aligned} \tag{19}$$

The probability matrix $\mathbf{P}$ is already determined by using Theorem 1. To find the stationary probability $\pi^{(0)}$, recall that the range of relative speed of two nodes is over $[0, 2(\bar{V}+\delta_V)]$. Hence, the maximum distance between a node-pair during each time step is $2(\bar{V}+\delta_V)$. This means the *maximum* number of states N of $\mathbf{P}$ can be traveled during one time step is,

$$N = \lceil\frac{2(\bar{V}+\delta_V)}{\varepsilon}\rceil. \tag{20}$$

In Fig. 2, when node w moves across node u's transmission zone, it may be at one of N possible states (from state S_n to S_{n-N+1}) at time t_0. Here we assume that node w initially lies in these N states with an equal probability as $1/N$ for determining the distribution $\pi^{(0)}$. Following (19) and (20), the PMF of link lifetime distribution is derived as:

$$\begin{aligned} &Prob\{T_L = m\} = Prob\{T_L \le m\} - Prob\{T_L \le m-1\} \\ &= [\pi^{(0)}\mathbf{P}^m]_{(n+1)} - [\pi^{(0)}\mathbf{P}^{m-1}]_{(n+1)}. \end{aligned} \tag{21}$$

In order to have a better understanding the above results, we simulate both the radio environments and smooth node mobility by ns-2. Specifically, upon (4), the value of ETR is chosen from the set $\{94m, 149m, 200m, 239m, 286m, 342m\}$, which are obtained by considering typical urban micro-cells ($3 \le \xi \le 3.5$) superimposed with shadow fading ($\sigma_s \in [6,9]dB$) [25].

Here, we carried out multiple trials with 50 nodes with $R_e = 239$ m, uniformly distributed in an area of 1401m $\times$1401m during a time period of 1000 seconds. The smooth user mobility [24] is set to zero pause time, 0.5 for temporal correlation parameter ζ, $[20, 40]$ seconds for the moving phase, and $[4, 6]$ seconds for acceleration and deceleration

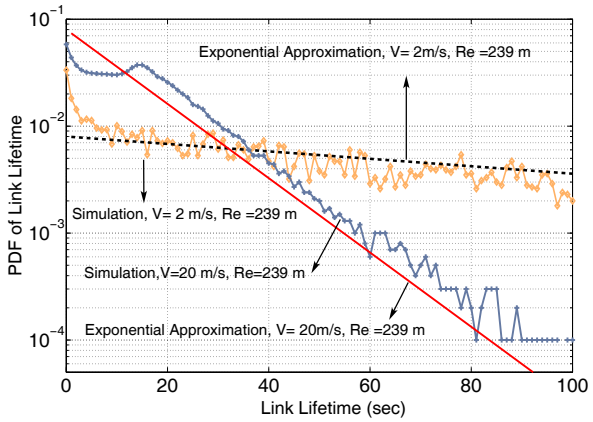

Fig. 4. Link lifetime distribution.

phases. Fig. 4 illustrates the link lifetime distribution with two mobility levels: low level ($\bar{V} = 2$ m/sec) and high level ($\bar{V} = 20$ m/sec). For clear demonstration, we show the results in the log-scale on Y-axis. The simulation results in Fig. 4 suggest that *link lifetime decreases exponentially with time regardless of the node speed and it decreases much quickly as the node speed is high.*

To verify our conjecture that link lifetime follows exponential distribution, we perform *chi-square goodness-of-fit* tests, which can evaluate to what extent the observed data and the hypothesis have a good fit. To begin with, we estimate the exponential distribution parameter $\lambda = E(T_L)$. Accordingly, the null-hypothesis H_0 is: the samples of link lifetime have exponential distribution with λ. Assume $k = 10$ intervals of Chi-square test with equal probability $1/10 = 0.1$, and significance level $\alpha = 0.05$. Since there is only one parameter in exponential distribution, the degree of freedom of chi-square test is 8. Referring to the table of critical chi-square value, we have $\chi^2_{0.05,8} = 16.919$. The end points of the 10 intervals can be obtained by $i_j = -\frac{ln(1-r_j)}{\lambda}$, where $r_j = 0.1 * j$ for $0 \leq j \leq 9$, and $i_{10} = \infty$ as $r_{10} = 1$. Based on samples with size $n = 100$, the chi-value can be calculate according to $\chi^2 = \sum_{j=1}^{k}(O(j) - E(j))^2/E(j)$, where $O(j)$ is number of data observed in interval j, i.e., link lifetime is between $[i_{j-1}, i_j]$, and $E(j)$ is the expected frequency for interval j, i.e., $E(j) = 0.1n$. We find that χ^2 values of samples with low or high mobility levels are less than critical chi-square value 16.919, i.e., the *Chi-Square Test accepts our hypothesis* H_0, which validates that link lifetime does follow exponential distribution.

Interestingly, by taking a close look, we find that the PMF of link lifetime distribution can be approximated by an exponential distribution with parameter $\frac{\bar{V}}{R_e}$, which will be discussed in detail in Section IV-A, that is,

$$f_{T_L}(t) \approx \frac{\bar{V}}{R_e} \cdot e^{(-\frac{\bar{V} \cdot t}{R_e})} = \frac{\bar{V}}{f(\xi, \sigma_s, \chi)} \cdot e^{(-\frac{\bar{V} \cdot t}{f(\xi, \sigma_s, \chi)})}. \quad (22)$$

The equation (22) in fact represents the PDF of link lifetime with continuous time t. It can be seen in Fig. 4 that this approximated exponential distribution characterized by the parameter $\frac{\bar{V}}{R_e}$, matches very well with the simulation results, especially for high speed. Recall, $R_e = f(\xi, \sigma_s, \chi)$, defined in (4), is a function of radio channel parameters: path loss (ξ), shadow fading (X_{σ_s}), and multi-path fading (χ^2). Hence, the parameter $\frac{\bar{V}}{R_e}$ in (22) indicates that the *link performance in mobile wireless network can be characterized by joint effects of radio channels and node mobility*.

TABLE I
COMPARISON: $\overline{T}_L(s)$ AND ESTIMATED $\hat{T}_L(s)$, FOR $R_e = 239$ M AND DIFFERENT AVERAGE SPEED $\bar{V}(m/sec)$.

$\bar{V}$	2	5	10	15	20	25
$\overline{T}_L$	112.94	50.75	24.89	19.23	15.72	12.68
$\hat{T}_L$	119.5	47.8	23.9	15.9	12.0	9.6

In addition, simulations under other mobility models, such as Gauss-Markov (GM) and Random WayPoint (RWP) model, suggest that smooth mobility with microscopic movement, such as smooth mobility and GM mobility, more likely follows exponential distribution. In contrast, unsmooth movement or purely randomness movement, such as RWP, does not follow exponential distribution. More details can be found in [31] Section 3.4.

Remark 4: The link lifetime distribution can be approximated by an exponential distribution with parameter $\frac{\bar{V}}{R_e}$, where $\bar{V}$ is the average speed and R_e is the ETR of a mobile node. This result is in contrast with previous studies that there exists a peak in the distribution function which are mainly obtained from random mobility models [3], [9], [11].

IV. Link Stochastic Properties

In this section, we discuss link properties such as average link lifetime, residual link lifetime, and link change rate. These link dynamics effectively reveal the changing frequency of network topology [6], [7], efficiency of routing operations [2], [4], and application performance in multihop wireless networks[9], [26].

A. Average Link Lifetime

From (21), the average link lifetime $\overline{T}_L$ is given by:

$$\overline{T}_L = \sum_{m=1}^{\infty} m([\pi^{(0)}\mathbf{P}^m]_{(n+1)} - [\pi^{(0)}\mathbf{P}^{m-1}]_{(n+1)}). \quad (23)$$

Interestingly, we find that the $\overline{T}_L$ can be estimated by the empirical equation $\hat{T}_L = R_e/\bar{V}$. Table I illustrates the results of both theoretical $\overline{T}_L$ from (23) and estimated $\hat{T}_L$ with respect to node mobility. The physical meaning of the equation $\hat{T}_L = R_e/\bar{V}$ is the time a node takes to move across the radius of its neighbor's transmission zone at its average speed $\bar{V}$. This result could be used as an engineering approximation of link lifetime in ad hoc networks, especially for low mobility to medium mobility with speed less than 35 km/hour.

Based on the theoretical results on (23), we further investigate the ETR effect on average link lifetime $\overline{T}_L$ with different node mobility. The results are shown in Fig. 5(a). We find that the larger R_e is, the longer the $\overline{T}_L$ is obtained, which is consistent with our expectation. However, it can be observed that the ETR has much more significant impact on $\overline{T}_L$ for nodes with low mobility than those with high mobility. For example, in the case of low mobility, i.e., the average

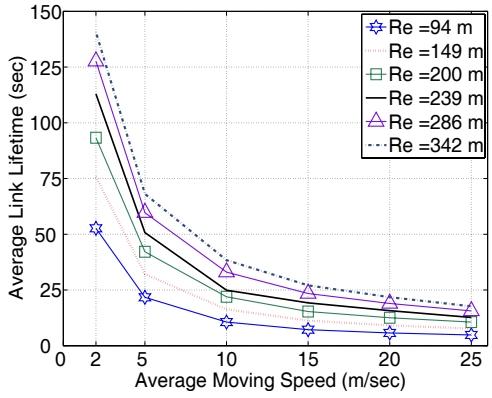

(a) Average link lifetime

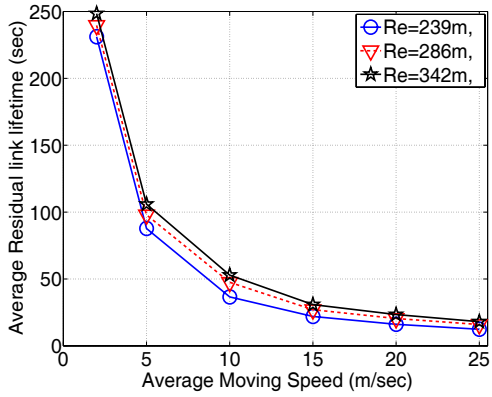

(b) Average residual link lifetime

Fig. 5. Stochastic properties of link lifetime and residual link lifetime.

node speed is 2 m/sec, $\overline{T}_L$ varies from 50 sec to around 125 sec when R_e increases from 94 m to 342 m, respectively. In contrast, when the node speed is high, at 25 m/sec, with the same range of R_e, the value of $\overline{T}_L$ varies within 20 sec.

Remark 5: For multihop wireless networks with lower node mobility, or even without node mobility such as static sensor networks, the average link lifetime $\overline{T}_L$ is predominated by ETR, i.e., radio channel characteristics. For a network with faster mobile nodes such as vehicular ad hoc networks, $\overline{T}_L$ is dominated by node speed.

B. Residual Link Lifetime

Residual link lifetime T_R is the remaining link duration after the link is established. It can be interpreted by link availability $L(\rho_m^{(i)}, m')$, which is a probability that a link will be continuously available at least m' steps given that the link exists m time steps with node-pair distance ρ_m in state S_i.

$$L(\rho_m^{(i)}, m') = \frac{Prob\{T_L \geq m' + m\}}{Prob\{T_L > m \mid \rho_m \in S_i\}}. \tag{24}$$

Therefore, upon the definition of link availability $L(\rho_m^{(i)}, m')$ in (24), the corresponding PMF of residual link lifetime T_R is represented as

$$\begin{aligned} Prob\{T_R = m'\} &= L(\rho_m^{(i)}, m') - L(\rho_m^{(i)}, m'+1) \\ &= [\pi_{i,1}^{(m)} \mathbf{P}^{m'+1}]_{(n+1)} - [\pi_{i,1}^{(m)} \mathbf{P}^{m'}]_{(n+1)}, \end{aligned} \tag{25}$$

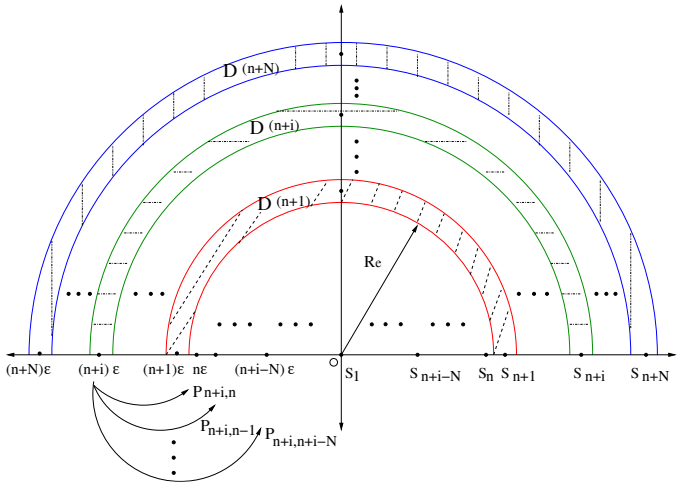

Fig. 6. Derivation of average link arrival rate λ.

where $\pi_{i,1}^{(m)}$ is a vector in which the i-th element is equal to 1, while other elements are equal to 0. The physical meaning of $\pi_{i,1}^{(m)}$ is after m-th time step, the probability of the node location is $Prob\{\rho_m \in S_i\} = 1$.

Next, given this initial 200 m node-pair distance, Fig. 5(b) illustrates the average residual link lifetime with respect to node mobility under different ETRs by simulations. It turns out the average residual link lifetime is much more sensitive to the node mobility than the transmission range. Compared to the results shown in Fig. 5(a), we also observe that the impacts of transmission range on the average residual link lifetime is very similar to that on the average link lifetime.

Remark 6: Similar to the link lifetime, the impacting factors on residual link lifetime are in the decreasing order of average node speed, ETR, and node-pair distance.

C. Link Change Rate and Link Arrival Rate

Radio links among nodes in multihop wireless networks have an immediate effect on network topology. In this section, we analyze the average link change rate, which is defined as the average number of link changes per second observed by a single node. According to Fig. 2, the total number of new mobile nodes moving into node u's transmission zone during time interval $[0, t]$ is $N_a(t)$, which denotes the total number of new link arrivals. And the total number of link breakages for the node u during time interval $[0, t]$ is $N_b(t)$. Then, we denote the *average link arrival rate* as $\lambda = \lim_{t\to\infty} \frac{N_a(t)}{t}$ and the *average link breakage rate* as $\mu = \lim_{t\to\infty} \frac{N_b(t)}{t}$, respectively. In [3], Samar et al. showed that the average link arrival rate λ is equal to the average link breakage rate μ in multihop wireless networks. Let η_L denote the *average link change rate*. Thus,

$$\eta_L = \lambda + \mu = 2\lambda. \tag{26}$$

Upon Fig. 2, the average link arrival rate λ is equivalent to the average number of new nodes entering node u's transmission zone at every time step. Thus, we extend the total number of states of matrix $\mathbf{P}$ from $n+1$ to $n+N$, where N is obtained in (20). The extended states are shown in Fig. 6. Hence, a node could enter node u's transmission

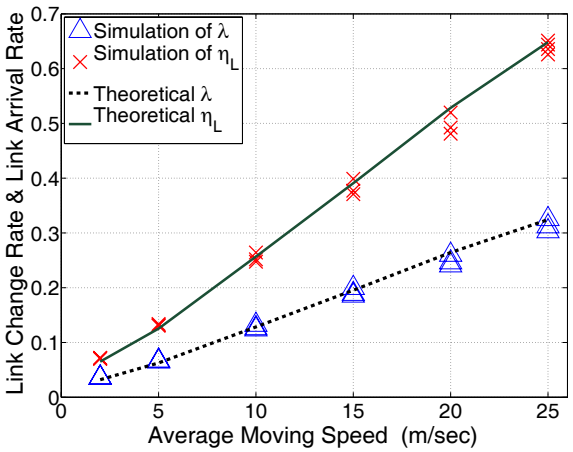

Fig. 7. Node mobility impacts λ.

zone at the next time step, only if it is currently lying in one of the states $\{S_{n+1}, S_{n+2}, ..., S_{n+N}\}$. Let $P_L(n+i)$ denote the probability that a node in state S_{n+i} will move into node u's transmission zone during the next time step movement. Then, $P_L(n+i)$ is given by:

$$P_L(n+i) = \sum_{j=n+i-N}^{n} P_{n+i,j} \quad , \quad 1 \le i \le N, \tag{27}$$

where $P_{n+i,j}$ can be obtained from the approximation equation (13). Furthermore, for S_{n+i}, we denote the region $\mathbf{D}_{n+i}$ as the the set of all positions that are in distance of $[(n+i-1)\varepsilon, (n+i)\varepsilon]$ away from the reference node u. This set actually covers the region of a circular ring with the outer radius $(n+i)\varepsilon$ and the inner radius $(n+i-1)\varepsilon$, respectively. Hence, we have the area of $\mathbf{D}_{n+i}$, $S(\mathbf{D}_{n+i}) = \pi\varepsilon^2[(n+i)^2-(n+i-1)^2] = \pi\varepsilon^2(2i+2n-1)$. Using the same assumption in [3], [6] that node density σ follows the uniform distribution, then $\sigma \cdot S(\mathbf{D}_{n+i})$ is the average number of nodes lying within $\mathbf{D}_{n+i}$. Therefore, the total number of possible nodes moving into node u's transmission zone at the next time step is the summation of the number of nodes currently lying at all possible regions $\mathbf{D}_{n+i}$, $1 \le i \le N$. Then, the average link arrival rate λ is represented as:

$$\begin{aligned}\lambda &= \sum_{i=1}^{N} P_L(n+i) \cdot \sigma \cdot S(\mathbf{D}_{n+i}) \\ &= \sigma\pi\varepsilon^2 \sum_{i=1}^{N} \sum_{j=n+i-N}^{n} P_{n+i,j} \cdot (2i+2n-1).\end{aligned} \tag{28}$$

To validate the analytical results of average link change rate η_L and average link arrival rate λ in (26) and (28), respectively, we compare the theoretical results with the simulation results according to different node speed in Fig. 7. As can be observed, the analytical results match the the simulation results very well. Thus, we validate that the average link change rate η_L is *two times* as large as the average new link arrival rate λ. Also, we find that given a fixed transmission change R_e, both η_L and λ grow almost linearly with the increase of the node speed.

V. Implications of Link Properties

The knowledge of link stochastic properties under different factors such as radio channel characteristics and node mobility offers deep insights on performance evaluation and improvements in multihop wireless networks. Next, we apply analytical results of link properties to investigate their implications on path lifetime, network connectivity and routing protocol optimization.

A. k-hop Path Lifetime

To study the path properties, it is generally assumed that the stochastic properties of different links incident to k-hop path are identical and links fail independently. Let each link lifetime in a k-hop path be $T_{L1}, T_{L2}, \ldots, T_{Lk}$, respectively. Then, the path duration time T^k_{path} is equivalent to the minimum duration time among its k incident links, i.e., $T^k_{path} = \min\{T_{Li} \mid 1 \le i \le k\}$ [3], [9]. Hence, given the CDF of link lifetime $F_L(m)$ derived in (19), then the CDF of path lifetime $F^k_{path}(m) = Prob\{T^k_{path} \le m\}$ is derived as:

$$\begin{aligned}F^k_{path}(m) &= 1 - Prob\{\min_{1\le i\le k} T_{Li} > m\} \\ &= 1 - [1 - F_L(m)]^k = 1 - [1 - \pi^{(0)}\mathbf{P}^m(n+1)]^k.\end{aligned} \tag{29}$$

Compared (19) with (29), the CDF of 1-hop path lifetime is exactly the CDF of link lifetime. Recall that in (22), we showed that the PMF of link lifetime distribution can be approximated by an exponential distribution with parameter $\frac{V}{R_e}$, which does not rely on the geographic information of a node pair. Since the path lifetime is determined by the minimum link lifetime en route, and assuming link fails independently, we can easily conclude that *the approximation of path lifetime PDF also follows exponential distribution with the parameter* λ^k_P [30]. This analysis greatly relaxes the assumption of large (approach to infinite) hop-count of a path for its distribution converging to exponential [17]. In particular, the parameter $\lambda^k_P = \sum_l^k \frac{\overline{V}_l}{R_{el}}$, where R_{el} and $\overline{V}_l$ are the associated ETR and average node speed for the l^{th} link along the k-hop path.

B. Network Connectivity

Now we apply the average link lifetime $\overline{T}_{link}$ and average link change rate η_L to investigate their impacts on average node degree, and further network connectivity. Let $\kappa(G(t))$ and $E\{d_{G(t)}\}$ be the network connectivity and average degree of a multihop wireless network $G(t)$, respectively. Then we have $\kappa(G(t)) \le E\{d_{G(t)}\}$. Thus, $E\{d_{G(t)}\}$ is the upper bound of the connectivity of $G(t)$. Let each node in $G(t)$ be associated with a queuing system. For instance, in the node u's system, an arrival event means the event that a node moves inside node u's transmission zone, and a departure event represents a node moves outside its transmission zone. Then, according to the Little's law of a queuing system: the average number of customers in the system , i.e., $E\{d_{G(t)}\}$, is equal to the average arrival rate of customer to the system, i.e., λ, multiplied by the average system time per customer, i.e., $\overline{T}_{link}$. Therefore, we can apply $\overline{T}_{link}$ in (23) and η_L in (26) and (28) to estimate the upper bound connectivity of a multihop wireless network,

$$\kappa(G(t)) \leq E\{d_{G(t)}\} = \lambda \cdot \overline{T}_{link} = \frac{1}{2}\eta_L \cdot \overline{T}_{link}. \qquad (30)$$

In fact, $E\{d_{G(t)}\}$ implies the maximum number of disjoint end-to-end paths available for a large dense multihop network. Therefore, the knowledge of $\kappa(G(t))$ and $E\{d_{G(t)}\}$ from (30) can benefit path selection and routing design especially for a large dense multihop network.

C. Routing Performance

The effective design of routing protocols should take into account the crucial factors such as wireless channel characteristics, node density and node mobility. As explained earlier in this paper, the complex interactions of these factors directly determine the link properties in a multihop network. Thus, the link properties such as average link lifetime can be utilized as the effective indicators of network performance and the metrics for designing mobility adaptive routing protocols [32].

In this section, we investigate the impacts of link dynamics on routing performance by taking AODV as a case study in ns-2. The network traffic is composed of 20 constant bit rate (CBR) sources and 30 connections among total 50 nodes. And each source sends 1 packet/sec with the packet size 64 bytes. The value of ETR is chosen from the set $\{94m, 149m, 200m, 239m, 286m, 342m\}$, which are obtained by considering typical urban micro-cells ($3 \leq \xi \leq 3.5$) superimposed with shadow fading ($\sigma_s \in [6, 9]dB$) [25]. From Fig. 8(a) and 8(b), it can be seen that the performance of average end-to-end packet delay and throughput increases substantially as the rise of ETR R_e. However, in Fig. 8(b) when $R_e \leq 239$m, the routing performance is not acceptable for practical applications, because of network dis-connectivity due to lack of neighboring nodes.

Interestingly, we find that the routing overhead increases when R_e rises from $[94, 286]$m, and it starts to reduce regardless of node speed when $R_e > 286$m. (Figure is not included because of page limit.) This is because the increasing number of neighboring nodes is large enough to almost always form a connected network, while dramatically reducing the number of path updates. Thus, we find that routing protocols should only be evaluated and studied under certain range of node density, where the statistics of link properties can be well applied to improve the routing efficiency as well as the network performance. For example, as shown in Fig. 8, for a network where the average node speed is 15 m/sec, it could be a typical vehicular ad hoc network in downtown area under both shadowing and small-scale fading. We found that the end-to-end throughput increases from 69% to 91% when the average node degree $E\{d_{G(t)}\}$ increases from 4.45 to 7.39 with the growth of ETR. Accordingly, under the same condition, the end-to-end packet delay drops from 0.43 sec to 0.12 sec. Thus, based on the simulation results in this study, we suggest that the routing performance varies sensitively with the variation of ETR. In particular, it can be effectively improved by applying the knowledge of link dynamics when the number of nodes per transmission zone, σ_R, changes from 3 to 10.

VI. Conclusions

In this paper, we presented a modeling approach to study the joint effects of radio channels and node mobility on link properties by using a transition probability matrix. We have found that i) radio channel characteristics predominate the link performance for slower mobile nodes, while node mobility dominates the link performance for faster mobile nodes; ii) link lifetime can be effectively approximated by exponential distribution with parameter $\frac{\bar{V}}{R_e}$; iii) the impacting factors on both link and residual link lifetime are in the decreasing order of average node speed $\bar{V}$, ETR, and node-pair distance; and iv) k-hop path lifetime can also be characterized by an exponential distribution for any arbitrary hop-count k. By demonstrating the implications of link properties on path lifetime, node degree, and routing performance, the proposed approach and results provided several new findings that can be readily applied to system design such as topology control and routing optimization.

References

[1] W. Wang and M. Zhao, "Joint effects of radio channels and node mobility on link dynamics in wireless networks," in *Proc. 2008 IEEE INFOCOM*.

[2] F. Bai, N. Sadagopan, B. Krishnamachari, and A. Helmy, "Important: a framework to systematically analyze the impact of mobility on performance of routing protocols for ad hoc networks," in *Proc. 2003 IEEE INFOCOM*.

[3] P. Samar and S. B. Wicker, "On the behavior of communication links of node in a multi-hop mobile environment," in *Proc. 2004 ACM MobiHoc*.

[4] Z. Cheng and W. Heinzelman, "Exploring long lifetime routing (LLR) in ad hoc networks," in *Proc. 2004 ACM International Symposium MSWiM*.

[5] A. Boukerche, "Performance evaluation of routing protocols for ad hoc wireless networks," *Kluwer Mobile Netw. Applications*, vol. 9, pp. 333–342, 2004.

[6] C. Bettstetter and C. Hartmann, "Connectivity of wireless multihop networks in a shadow fading environment," *ACM/Kluwer Wireless Netw.*, vol. 11, no. 5, pp. 571–579, Sep. 2005.

[7] D. Miorandi and E. Altman, "Coverage and connectivity of ad-hoc networks in presence of channel randomness," in *Proc. 2005 IEEE INFOCOM*.

[8] P. Santi, *Topology Control in Wireless Ad Hoc and Sensor Networks*. Wiley, 2006.

[9] N. Sadagopan, F. Bai, B. Krishnamachari, and A. Helmy, "Paths: analysis of path duration statistics and their impact on reactive MANET routing protocols," in *Proc. 2003 ACM MobiHoc*.

[10] M. Qin, R. Zimmermann, and L. S. Liu, "Supporting multimedia streaming between mobile peers with link availability prediction," in *Proc. 2005 ACM International Conf. Multimedia*.

[11] M. Gerharz, C. Waal, M. Frank, and P. Martini, "Link stability in mobile wireless ad hoc networks," in *Proc. 2002 IEEE Local Computer Networks*.

[12] X. Wu, H. R. Sadjadpour, and J. J. Garcia-Luna-Aceves, "An analytical framework for the characterization of link dynamics in manets," in *Proc. 2006 IEEE MILCOM*.

[13] S. Xu, K. Blackmore, and H. Jones, "Assessment for MANETs requiring persistent links," in *Proc. 2005 International Workshop WitMeMo*.

[14] X. Hong, T. J. Kwon, M. Gerla, D. L. Gu, and G. Pei, "A mobility framework for ad hoc wireless networks," in *Proc. 2001 International Conf. Mobile Data Management*.

[15] A. B. McDonald and T. F. Znati, "A mobility-based framework for adaptive clustering in wireless ad hoc networks," *IEEE J. Sel. Areas Commun.*, vol. 17, no. 8, pp. 1466–1487, Aug. 1999.

[16] S. Jiang, "An enhanced prediction-based link availability estimation for MANETs," *IEEE Trans. Commun.*, vol. 52, no. 2, pp. 183–186, Feb. 2004.

[17] R. J. La and Y. Han, "Distribution of path durations in mobile ad-hoc networks and path selection," in *Proc. 2006 IEEE INFOCOM*.

[18] J.-K. Lee and J. C. Hou, "Modeling steady-state and transient behaviors of user mobility: formulation, analysis, and application," in *Proc. 2006 ACM MobiHoc*, pp. 85–96.

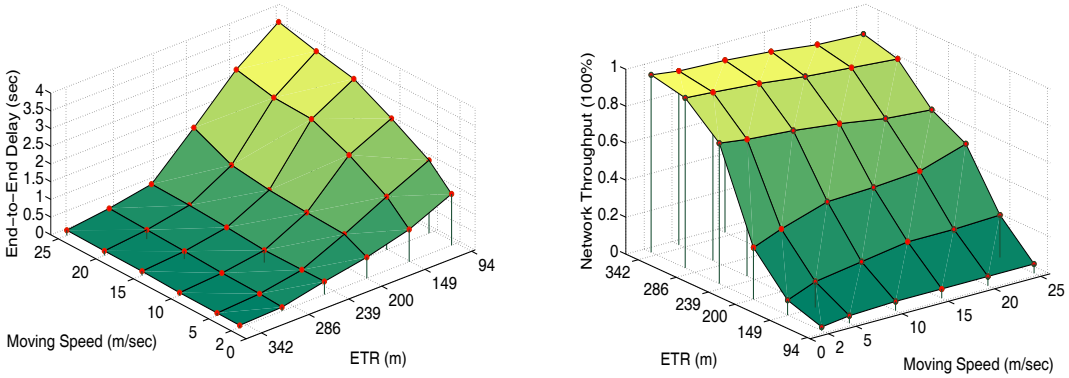

(a) Average packet delay.

(b) Network throughput.

Fig. 8. Effective transmission range and node mobility impacts on AODV routing performance.

[19] I. Rhee, M. Shin, S. Hong, K. Lee, and S. Chong, "On the Levy-Walk nature of human mobility," in *Proc. 2008 IEEE INFOCOM*.

[20] T. Karagiannis, J.-Y. LeBoudec, and M. Vojnovic, "Power law and exponential decay of inter contact times between mobile devices," in *Proc. 2007 ACM MOBICOM*, pp. 183–194.

[21] X. Zhang, J. Kurose, B. Levine, D. Towsley, and H. Zhang, "Study of a bus-based disruption-tolerant network: mobility modeling and impact on routing," in *Proc. 2007 ACM MOBICOM*, pp. 195–206.

[22] C. Bettstetter, "Mobility modeling in wireless networks: categorization, smooth movement, and border effects," in *ACM Mobile Computing Commun. Rev.*, vol. 5, no. 3, 2001.

[23] T. Camp, J. Boleng, and V. Davies, "A survey of mobility models for ad hoc networks research," *Wireless Commun. Mobile Computing*, vol. 2, no. 5, pp. 483–502, 2002.

[24] M. Zhao and W. Wang, "A unified mobility model for analysis and simulation of mobile wireless networks," *ACM-Springer Wireless Networks*, vol. 15, no. 3, pp. 365–389, Apr. 2009.

[25] M. Schwartz, *Mobile Wireless Commnications*, 1st edition. Cambridge University Press, 2005.

[26] C. E. Koksal, K. Jamieson, E. Telatar, and P. Thiran, "Impacts of channel variability on link-level throughput in wireless networks," in *Proc. 2006 SIGMetrics Performance*.

[27] L. Booth, J. Bruck, M. Cook, and M. Franceschetti, "Ad hoc wireless networks with noisy links," in *Proc. 2003 IEEE ISIT*.

[28] M. Gerharz, C. Waal, P. Martini, and P. James, "Strategies for finding stable paths in mobile wireless ad hoc networks," in *Proc. 2003 IEEE Local Computer Networks*, pp. 130–139.

[29] "Accutech: factors affecting transmission distance." Available: http://www.accutechinstruments.com/downloads/technical-articles/tech-note-215-transmission-distance.pdf

[30] A. Papoulis, *Probability, Random Variables, and Stochastic Processes*. McGraw-Hill, 1991.

[31] M. Zhao and W. Wang, "Design, modeling, and analysis of user mobility and its impact on multi-hop wireless networks," Ph.D. dissertation, North Carolina State University, 2009.

[32] J. Boleng, W. Navidi, and T. Camp, "Metrics to enable adaptive protocols for mobile ad hoc networks," in *Proc. 2002 ICWN*, pp. 293–298.

Ming Zhao received his B.S. in electrical engineering from Harbin Institute of Technology in 1997. He received the M.S.E.E. from New York State University at Buffalo in 2004, and his Ph.D. degree from North Carolina State University in 2009, respectively. His research interests are in mobility modeling, user mobility, network performance and management in wireless networks, and video multicast routing in IP networks. Ming Zhao has worked as a software engineer for Cisco Systems at the RTP campus since 2008.

Yujin Li received her B.S. and M.S. degrees in control science and engineering from Beijing Institute of Technology, Beijing, China, in 2007 and 2009, respectively. She is currently a Ph.D. student in the Department of Electrical and Computer Engineering at North Carolina State University. Her research interest is mobility modeling and management in wireless networks.

Wenye Wang received the B.S. and M.S. degrees from Beijing University of Posts and Telecommunications, Beijing, China. She also received the M.S.E.E. and Ph.D. degrees from the Georgia Institute of Technology, Atlanta, Georgia, in 1999 and 2002, respectively. She is an Associate Professor with the Department of Electrical and Computer Engineering at North Carolina State University. Her research interests are in mobile and secure computing, network topology and architecture, and smart grid. Dr. Wang received the NSF CAREER Award in 2006. She is a senior member of IEEE.